Brain white matter damage and its association with neuronal synchrony during sleep

Erlan Sanchez[1,2], Héjar El-Khatib[1,3], Caroline Arbour[1,4], Christophe Bedetti[1,5], Hélène Blais[1], Karine Marcotte[1,6], Andrée-Ann Baril[1,7], Maxime Descoteaux[8], Danielle Gilbert[1], Julie Carrier[1,3], Nadia Gosselin[1,3]

[1]Research center of the Hôpital du Sacré-Coeur de Montréal, Qc, Canada.
[2]Département de Neurosciences, Université de Montréal, Qc, Canada.
[3]Department de psychologie, Université de Montréal, Qc, Canada.
[4]Faculté de sciences infirmières, Université de Montréal, Qc, Canada
[5]Research center of the Institut universitaire de gériatrie de Montréal, Qc, Canada
[6]École d'orthophonie et d'audiologie, Université de Montréal, Qc, Canada
[7]Département de psychiatrie, Université de Montréal, Qc, Canada
[8]Département d'informatique, Université de Sherbrooke, Qc, Canada

Running head: Sleep synchrony and white matter

Published in: Brain

Number of words: 5391

Number of words (abstract) 341

Corresponding author:
Nadia Gosselin, Ph.D.
Center for Advanced Research in Sleep Medicine
Hôpital du Sacré-Cœur de Montréal
5400 boul. Gouin Ouest, local E-0330, Montréal, Québec,
H4J 1C5, Canada
Tel: 514-338-2222 ext. 7717; Fax: 514-338-3893
Email: nadia.gosselin@umontreal.ca

Abstract

The restorative function of sleep partly relies on its ability to deeply synchronize cerebral networks to create large slow oscillations observable with electroencephalography. However, whether a brain can properly synchronize and produce a restorative sleep when it underwent massive and widespread white matter damage is unknown. Here, we answered this question by testing twenty-three patients with various levels of white matter damage secondary to moderate to severe traumatic brain injuries (ages 18-56; 17 males, 6 females, 11-39 month post-injury) and compared them to twenty-seven healthy subjects of similar age and sex. We used magnetic resonance imaging and diffusion tensor imaging metrics (e.g. fractional anisotropy as well as mean, axial and radial diffusivities) to characterize voxel-wise white matter damage. We measured the following slow wave characteristics for all slow waves detected in N2 and N3 sleep stages: negative and positive phase durations, peak-to-peak amplitude, negative-to-positive slope, and slow wave density. Correlation analyses were performed in traumatic brain injury and control participants separately, with age as a covariate. Contrary to our hypotheses, we found that greater white matter damage mainly over the frontal and temporal brain regions was strongly correlated with a pattern of higher neuronal synchrony characterized by slow waves of larger amplitudes and steeper negative-to-positive slopes during non-rapid eye movement sleep. The same pattern of associations with white matter damage was also observed with markers of high homeostatic sleep pressure. More specifically, higher white matter damage was associated with higher slow-wave activity power, as well as with more severe complaints of cognitive fatigue. These associations between white matter damage and sleep were found only in our traumatic brain injured participants, with no such correlation in controls. Our results suggest that, contrary to previous observations in healthy controls, white matter damage doesn't prevent the expected high cerebral synchrony during sleep. Moreover, our observations challenge the current line of hypotheses that white matter microstructure deterioration reduces cerebral synchrony during sleep. Our results showed that the relationship between white matter and the brain's ability to synchronize during sleep is neither linear nor simple.

Keywords

White matter; Sleep; NREM sleep; Traumatic brain injury

Abbreviations

DTI, diffusion tensor imaging

EEG, electroencephalography

GCS, Glasgow Coma Scale

MRI, magnetic resonance imaging

NREM, non-rapid eye movement

PSG, polysomnography

TBI, traumatic brain injury

Introduction

When the brain departs from wakefulness to enter into deep sleep, it shifts from a state of desynchronized electroencephalographic (EEG) activity to an avalanche of spontaneous slow (< 1 Hz) and large amplitude (> 75 μV) waves. These epiphenomena reflect slow oscillations that occur at a cellular level where intense and synchronized neuronal firing alternates with a period of silent state. Although cortically generated, slow waves are thought to emerge from the dynamic interplay between thalamic nuclei and the cerebral cortex (Murphy *et al.*, 2009; Crunelli *et al.*, 2015). They play crucial roles in the restorative properties of sleep, being notably essential to synaptic plasticity underlying learning and memory consolidation (Marshall *et al.*, 2006; Steriade, 2006; Tononi and Cirelli, 2006; Diekelmann and Born, 2010). Recent studies also implicate them with the clearance of neurotoxic waste products accumulated during wakefulness, a process thought to be compromised in some neurodegenerative diseases (Xie *et al.*, 2013; Mander *et al.*, 2015; Morawska *et al.*, 2016).

Current hypotheses suggest that the structural properties of white matter tracts affect how brain networks will synchronize themselves to produce slow oscillations during non-rapid eye movement (NREM) sleep. In one study, inter-individual differences of the corpus callosum volume explained 38% of NREM EEG slow-wave activity variability (Buchmann *et al.*, 2011). More specifically, larger volumes were associated with higher slow-wave activity power, supporting the hypothesis that large interhemispheric white matter tracts increase EEG synchronicity. In a second study, a steeper rising slope of the sleep slow waves, suggestive of a better cortical synchrony, was associated with a higher axial diffusivity in major frontal bundles, which the authors have associated with better white matter integrity (Piantoni *et al.*, 2013). Taken together, these results support the idea that healthier white matter tracts correlate with higher cerebral synchronicity during sleep.

However, these previous studies on cerebral white matter and sleep slow waves have been performed in young, healthy adults who probably have very little inter-individual variability in their white matter tracts. The question remains as to whether a brain can properly

synchronize its networks to produce large sleep slow waves and a restorative sleep when it underwent massive white matter damage, as seen in some neurological conditions. This question can be answered by testing patients with extensive white matter damage months after a moderate to severe traumatic brain injury (TBI). In fact, this population is particularly interesting to study, as most of these patients have visible white matter damage on magnetic resonance imaging (MRI) and up to 70% of them develop severe fatigue and chronic sleep disturbances, including increased sleep needs and reports of non-restorative sleep (Duclos *et al.*, 2014; Ouellet *et al.*, 2015). The inability of the brain to synchronize its local neuronal networks during sleep could be a key element to explain these complaints.

Here we investigated morphological characteristics of NREM sleep slow waves in individuals with various degrees of white matter damage secondary to moderate to severe TBI compared with healthy controls. We also performed correlational analyses between white matter structural properties in TBI subjects and sleep slow wave characteristics that are typically associated with neuronal synchrony. We tested the hypothesis that more severe white matter damage is associated with reduced neuronal synchrony during sleep (e.g. reduced slow wave amplitudes and slopes), which could impede the restorative function of sleep, and in doing so, generate the often observed fatigue and sleep disturbances.

Chronic TBI patients and controls completed daily sleep diary and wore an actimetric device the week preceding testing in order to monitor total sleep time the week before the MRI scanning and the PSG recording. All participants underwent a 3 Tesla MRI followed by a full night of in-laboratory polysomnography (PSG) the same day. The next morning, a comprehensive neuropsychological assessment was performed, and participants filled out questionnaires on mood, fatigue and sleep. To characterise white matter structure, we used diffusion tensor imaging (DTI), a technique that measures the diffusion of water molecules in the brain. Due to the clear directionality of white matter tracts, water diffusion is greater along the axis of the fibers and lower perpendicular to them, which allows inferring on axonal and myelin damage. We used four diffusion metrics namely fractional anisotropy, mean, axial and radial diffusivities to infer whole-brain voxel-wise white matter structure. In the case of severe damage to the white matter, as seen in chronic TBI patients, it is

expected to observe an increased diffusivity along axial and radial axes and a reduced fractional anisotropy(Kraus *et al.*, 2007; Kennedy *et al.*, 2009; Kumar *et al.*, 2009; Pitkonen *et al.*, 2012; Haberg *et al.*, 2015). To characterize NREM sleep slow waves, we used an automatic detection on a full night of PSG recording. We measured slow wave density and morphological characteristics, including amplitude, frequency, slope, and phase duration. We hypothesized that the extent of white matter damage (reflected by increased diffusivities and reduced fractional anisotropy) predicts lower neuronal synchrony during sleep (reflected by waves of lower amplitude and slopes).

Methods

Participants

Twenty-three participants aged between 18 and 56 years old and diagnosed with a moderate to severe TBI were recruited for this prospective study and were compared to twenty-seven age- and sex-matched healthy controls. All TBI patients were previously admitted to the *Hôpital du Sacré-Coeur de Montréal*, a tertiary trauma center, in the acute stage of their injury and they were all recruited based on their hospital chart. During testing, TBI patients were in the chronic phase of the injury, at least 11 months following the trauma (average: 23.4 months, range 11-39 months, see Table 1 for demographic and clinical characteristics). Diagnosis of TBI, defined as an alteration in brain function, or other evidence of brain pathology, caused by an external force (Menon *et al.*, 2010), was performed by a licensed neurosurgeon according to standard established criteria for moderate to severe TBI (Teasdale and Jennett, 1974): a Glasgow Coma Scale (GCS) score between 3 and 12, a post-traumatic amnesia longer than 1 h, a loss of consciousness longer than 30 min, and positive brain scans. All participants presenting any of the following conditions were excluded from the study: (1) a history of psychiatric, neurologic, sleep (before the injury), or substance use disorders; (2) sleep medication and inability to cease medication use prior to testing; (4) history of single (for control subjects) or multiple TBI (for TBI patients); (5) quadriplegia; (6) obesity, defined by a body mass index over 30; (7) pregnancy; (8) jetlag due to a recent trans-meridian trip; (9) night shift work leading to an atypical sleeping schedule; (10) MRI contraindications (often in the form of metallic implants left by surgeries). Eight TBI

participants were taking psychoactive medication prior to recruitment (see Supplementary Table I for detailed data). Of those, three ceased the intake several days before the testing. The medicated patients, when compared to the rest of the group, showed no significant differences in either slow waves, sleep quality, or fatigue scores and were therefore included in analyses. The study was approved by the *Hôpital du Sacré-Coeur de Montréal* Research Ethics Board and written consent was obtained from each participant or the immediate family (for inapt participants), compliant with the Declaration of Helsinki.

Overview of the Protocol

One week before the lab visit, participants wore an activity monitor device (Actiwatch-L or Actiwatch-Spectrum, Philips Healthcare, Andover, MA) and filled out a daily sleep diary to document their sleep-wake cycle. Participants then underwent a brain MRI followed by a full night of in-laboratory PSG the same day. A comprehensive neuropsychological assessment was performed the morning after PSG to measure executive functions, processing speed, attention, language, working memory, and global functioning. We collected clinical data related to the injury from their hospital charts. Participants also filled out several questionnaires: the Pittsburgh Sleep Quality Index (Buysse *et al.*, 1989), the Fatigue Severity Scale (Krupp *et al.*, 1989), the Epworth Sleepiness Scale (Johns, 1991), the Beck Anxiety Inventory (Beck *et al.*, 1988), and the Beck Depression Inventory-II (Beck *et al.*, 1996).

Polysomnography

Bedtime and wake time were determined according to the participant's usual schedule. The recording montage comprised nineteen EEG derivations (FP1, FP2, Fz, F3, F4, F7, F8, Cz, C3, C4, Pz, P3, P4, O1, O2, T3, T4, T5, T6), bilateral electrooculogram, chin and tibia electromyogram, and electrocardiogram. Nasal and oral airflows were measured using a pressure transducer, a thoracic belt, and an abdominal belt. Blood oxygen saturation was measured with a pulse oximeter on the finger. Sleep stages and events were scored according to criteria from the American Academy of Sleep Medicine scoring manual and sleep cycles according to the criteria of Aeschbach and Borbely (Aeschbach and Borbely, 1993).

Slow waves detection and analysis

Slow waves were detected automatically on selected frontal and central derivations (F3, F4, Fz, C3, C4, Cz) during NREM N2 and N3 sleep stages for all sleep cycles. Epochs containing artefacts were excluded by automatic and visual detection. These data were analyzed using an in-house software package combined with an acquisition software (Harmonie Stellate Systems, Montreal, Canada). EEG data were initially band pass filtered between 0.3 and 4.0 Hz with a linear phase finite impulse response filter (-3 dB). The criteria used for slow wave detection were: (1) negative peak lower than -40 μV; (2) peak-to-peak amplitude higher than 75 μV; (3) negative phase duration between 125 and 1500 ms; and (4) positive phase duration lower than 1000 ms (Carrier *et al.*, 2011). The following morphological characteristics were then identified for each slow wave detected: amplitude (voltage difference between the negative and positive peaks in μV), frequency (oscillation speed in Hz), slope (velocity of the change between the negative and positive peaks in μV/s), negative phase duration (in s), positive phase duration (in s), and density (number of slow waves per minute). A visual representation of these characteristics can be seen in Supplementary Fig. 1.

Slow-wave activity power

Quantitative EEG analysis was performed on the frontal derivations during NREM N2 and N3 sleep stages of the entire night and for sleep cycles 1 to 3 separately. Epochs containing artefacts were excluded by automatic and visual detection. These data were analyzed using an in-house software package combined with an acquisition software (Harmonie Stellate Systems, Montreal, Canada). Fast Fourier Transform was carried out on epochs of 5 seconds, and the absolute and relative (*delta / (theta+alpha+beta)*) power for the delta frequency band (0.5 – 4 Hz) was then calculated.

MRI acquisition

Magnetic resonance imaging of the brain was performed on a 3.0 T scanner (Siemens Magnetom Trio) at the *Unité de Neuroimagerie Fonctionnelle* of the *Institut universitaire de gériatrie de Montréal*. The MRI protocol consisted of a pulsed spin echo diffusion-weighted imaging sequence (echo-planar imaging) (64 non-collinear directions, image resolution = 2 x 2 x 2 mm^3, 72 slices, RT = 9500 ms, ET = 93 ms, b-value = 1000 s/mm^2, duration = 648 s)

with additional gradient field maps and AP/PA b0 sequences, a T1-weighted sequence (image resolution = 1 x 1 x 1 mm3, RT = 2530 ms, ET = 1.64 ms, duration = 363 s), a T2-weighted sequence and a FLAIR sequence. A licensed neuroradiologist inspected all MRI.

DTI preprocessing and analysis

Diffusion data were preprocessed using the Toolkit for Analysis in Diffusion MRI (http://unf-montreal.ca/toad/). The pipeline involves the following steps: (1) parcellation using the Freesurfer (https://surfer.nmr.mgh.harvard.edu/) recon-all pipeline v5.3.0; (2) denoising; (3) motion and distortion correction; (4) upsampling and registration with the parcelled anatomical images and atlases; (5) FSL tensor reconstruction; and (6) extraction of tensor metrics including fractional anisotropy and mean, axial and radial diffusivity.

Data were then prepared for the voxel-wise statistical analysis using TBSS (Smith *et al.*, 2006) from the FSL diffusion toolbox (https://fsl.fmrib.ox.ac.uk/) (Smith *et al.*, 2004). First, all subjects' fractional anisotropy data were affine-aligned to the MNI152 1mm standard space using the nonlinear registration tool FNIRT. Next, the mean fractional anisotropy image was created and thinned with a threshold of FA > 0.2 to create a mean fractional anisotropy skeleton which represents the centres of all tracts common to the group. Each subject's aligned fractional anisotropy data was then projected onto this skeleton. Similar steps were subsequently performed to project the mean, axial, and radial diffusivity data onto this skeleton as well.

Statistical analyses

The TBI and control groups were first compared on demographic characteristics, questionnaires, neuropsychological tests, and sleep macro-architecture using two-tailed Student t-tests or Chi-square. For slow wave analysis, in order to reduce the number of variables and because no hemisphere effect was observed, we pooled frontal electrodes together (frontal cluster: F3, F4, Fz) and central electrodes together (central cluster: C3, C4, Cz). For three participants, one electrode had to be removed due to artefacts, and we therefore used the two remaining electrodes only. One participant had all central electrodes removed, and was excluded from this analysis. To characterize slow waves in TBI and control

subjects, we performed repeated measure ANOVAs with one inter-subject factor (group: TBI versus control) and one repeated measure (electrode: frontal and central clusters), with age as a covariate to account for its effect on slow waves. These statistical analyses were carried out with SPSS Statistics version 20 (IBM Corp., 2011), with statistical significance set at $p<0.05$.

DTI statistics were performed using Randomise (Winkler *et al.*, 2014), a tool from the FSL diffusion toolbox. It uses nonparametric Monte Carlo permutation inference to perform voxel-wise statistics on the white matter images processed previously by TBSS. For each contrast of interest in our models, 10 000 permutations were done, giving us a confidence limit of ± 0.0044 for $p=0.05$. Threshold-free cluster enhancement was used as a thresholding method (Smith and Nichols, 2009; Winkler *et al.*, 2014). This method takes the raw statistic image and produces an output image in which the voxel-wise values represent the amount of cluster-like local spatial support. The family-wise error rate was accounted for by the Monte Carlo permutation test and the threshold-free cluster enhancement. Group comparisons were performed for fractional anisotropy, as well as for mean, axial, and radial diffusivities. Group correlations were performed on all four diffusion metrics for the following regressors with age as a confound variable: injury severity (Glasgow Coma Scale score, length of posttraumatic amnesia), slow wave characteristics from the frontal pool of electrodes (amplitude, slope, negative phase duration, positive phase duration, frequency, density), slow-wave activity power for F3 electrode (both relative and absolute, for sleep cycles 1 to 3 separately) and questionnaire scores. Regression analyses were performed in the TBI and the control groups separately. The significant clusters were labelled according to the ICBM-DTI-81 white matter atlas (Mori *et al.*, 2008). T-values of significant clusters were presented in the figures by masking the original t-value images to only show significant clusters ($p<0.05$ corrected for multiple comparisons). While all analyses were performed on the mean fractional anisotropy skeleton, significant clusters in the presented figures were filled from the thin fractional anisotropy skeleton to the mean fractional anisotropy image to better represent actual white matter.

Data availability

Relevant data that support the findings of this study are available from the corresponding author upon reasonable request.

Results

Participant characteristics

Demographic characteristics as well as questionnaire, neuropsychological and sleep macro-architecture results for both groups are presented in Table 1. The TBI group reported significantly more fatigue and worse sleep quality than controls. Additionally, these patients presented impairments in several cognitive domains, as evidenced by poorer performances than controls on neuropsychological tests. TBI patients' sleep macro-architecture was not different from controls despite their subjective evaluation of poor sleep quality and daytime fatigue. No group difference was found in the total sleep time measured with sleep diaries and actigraphy in the week preceding the PSG.

A voxel-wise statistical analysis (using Tract-Based Spatial Statistics from the FMRIB Software Library diffusion toolbox) of the preprocessed DTI scans showed extensive white matter damage in the TBI group (Fig. 1). Decreased fractional anisotropy and increased mean, axial and radial diffusivities were evident across almost all major white matter tracts in the brain, from the cerebral hemispheres to the brainstem. Furthermore, the TBI group was very heterogeneous in terms of white matter damage, with some individuals showing no difference from controls and others showing important sequelae. This extensive white matter damage was strongly correlated with markers of TBI severity, most notably the Glasgow Coma Scale scores upon hospital admission and post-traumatic amnesia duration (Supplementary Fig. 2).

Sleep slow waves in TBI participants compared to healthy controls

We first performed ANOVAs with Group and one repeated measure (EEG electrodes: frontal and central clusters) with age as a covariate on slow wave characteristics. We found no Group X EEG electrode interaction for any of the slow wave characteristics, but we observed several significant group effects (Table 2). TBI participants had slightly longer negative and

positive phase duration than control participants. As expected by the latter result, slow wave frequency was lower in TBI compared to control subjects. Finally, the negative-to-positive slope was lower in the TBI group compared to the control group. No significant main group effect was found for either slow wave amplitude or density.

Sleep slow waves and white matter damage

The analysis of white matter with voxel-wise statistics (using TBSS and Randomise from the FSL diffusion toolbox) revealed a pattern of strong associations with slow waves' morphology involving the amplitude, slopes, and negative phase duration. While no relationship was found in the control group, DTI metrics generally associated with a more damaged white matter predicted higher cortical synchrony during sleep in the TBI group.

Higher slow wave amplitude correlated with more severe white matter damage in TBI patients (Fig. 2), and more specifically with higher axial diffusivities in multiple voxel clusters in the frontal and temporal regions, involving the genu of the corpus callosum, the anterior and posterior limbs of the internal capsule, the retrolenticular part of the internal capsule, the anterior, posterior, and superior corona radiata, the posterior thalamic radiation, the inferior longitudinal and fronto-occipital fasciculus, the external capsule, the fornix, and the uncinate fasciculus (Fig. 2b). Higher slow wave amplitude also correlated with both higher radial diffusivities and higher mean diffusivities in the inferior, middle, and superior cerebellar peduncles (Fig. 2a,c).

Steeper slow wave slope was also correlated with more severe white matter damage in TBI patients. Namely, the negative-to-positive slope was steeper when axial diffusivity was higher in clusters located over the frontal and temporal regions that were previously detailed (Fig. 3).

The negative phase duration of the slow wave was also positively correlated with white matter damage in TBI patients (Fig. 4). More specifically, longer negative phases correlated with lower fractional anisotropy in multiple voxel clusters once again scattered in a fronto-temporal manner and involving the splenium of the corpus callosum, the cerebral peduncle,

the posterior limb of the internal capsule, the retrolenticular part of the internal capsule, the anterior and posterior corona radiata, the posterior thalamic radiation, the inferior longitudinal and fronto-occipital fasciculus, the external capsule, the fornix, the uncinate fasciculus, and the tapetum (Fig. 4a). Longer negative phases were also associated with higher mean diffusivities in the genu and body of the corpus callosum, and the anterior corona radiata (Fig. 4b).

In summary, in TBI patients, widespread white matter damage in various regions containing short and long-range white matter tracts was associated with a pattern of higher neuronal synchrony in which the sleep slow waves are of higher amplitude and steeper slopes. Longer negative phase duration was also associated with the same observed white matter damage.

Sleep slow-wave activity and white matter damage

To further investigate the association between cortical synchrony during sleep and white matter structure, we analyzed the NREM slow-wave activity power (0.5 to 4 Hz frequency band). We measured the absolute and relative slow-wave activity power for each sleep cycle. No group difference was found for NREM slow-wave activity power between TBI patients and controls for any of the sleep cycles. However, the voxel-wise correlations with DTI metrics showed very strong associations in the TBI group only, similar to what was found with slow waves voxel-wise analyses. More specifically, white matter damage was positively correlated with relative slow-wave activity power in the first sleep cycle only (Fig. 5) and with absolute slow-wave activity power in the second (Supplementary Fig. 3) and third sleep cycles (Supplementary Fig. 4). In these cases, higher relative and absolute slow-wave activity power correlated with higher mean diffusivities, higher radial diffusivities, and lower fractional anisotropy in regions mostly overlapping with what was found with slow waves' morphology analysis.

Subjective sleep quality, fatigue, and white matter damage

Finally, we set out to see if the variability in white matter structure had any relationship with self-reported measures of sleep and fatigue. In the TBI group, while sleep quality and daytime sleepiness did not correlate with white matter characteristics, fatigue was positively

correlated with white matter damage. Indeed, higher self-reported fatigue strongly correlated with higher axial diffusivities in the same pattern of voxel clusters mentioned previously (Fig. 6). No such associations were found for the control group. For both groups, no significant associations were found between any of the self-reported measures of sleep and fatigue and slow wave characteristics.

Discussion

In the present study, patients with moderate to severe TBI had widespread white matter damage throughout the brain, from all cortical tracts to the brainstem, which is consistent with the literature showing white matter damage in chronic TBI (Benson *et al.*, 2007; Kraus *et al.*, 2007; Kennedy *et al.*, 2009; Kinnunen *et al.*, 2011; Spitz *et al.*, 2013; Haberg *et al.*, 2015). Our DTI results suggest significant demyelination, axonal injury and white matter degeneration consecutive of moderate to severe TBI. Not surprisingly, the extent of white matter damage correlated with more severe TBI in our sample. Our most important result was that this white matter damage was strongly associated with signs of better neuronal synchrony during NREM sleep: EEG slow waves were of higher amplitude and had steeper slopes in participants with more damaged brains. These results are in opposition with our hypotheses, as we expected that a loss of white matter would have decreased neuronal synchrony and consequently, decreased slow wave slopes and amplitudes. Our results also showed that white matter damage correlated positively with longer slow wave negative phase, higher NREM sleep slow-wave activity power and more severe fatigue during the day. These results challenge our understanding of what represents healthy NREM sleep slow waves.

The complex relationship between cortical synchrony during sleep and white matter integrity

During NREM sleep, the brain is highly synchronized locally and spontaneously produces slow waves on the EEG. These epiphenomena reflect slow oscillations that occur at a cellular level, where periods of silent state (negative phase) alternate with intense synchronized neuronal firing (positive phase). The slow wave N-to-P slope represents the rate of transition

between the negative and the positive phases; steeper slopes are the result of a more synchronous transition between the silent phase to the depolarization phase. Slow wave amplitude, on the other hand, most likely represents the extent of the synchronal neuronal firing. The more cortical neurons are simultaneously depolarized, the larger the measured amplitude should be on the EEG. Slow oscillations occur across the cortex, originating mostly near the insula and the medial cingulate gyrus (Murphy *et al.*, 2009) from the dynamic interplay between thalamic nuclei and the cerebral cortex (Crunelli *et al.*, 2015), and propagate along the anterior-posterior axis of the brain through the cingulate pathways and parts of the default-mode network (Massimini *et al.*, 2004; Murphy *et al.*, 2009). Short- and long-range connections are therefore considered crucial for slow wave generation and propagation, and as such, a strong association with white matter is to be expected.

In line with this hypothesis, a previous study found that a steeper rising slope of slow waves was associated with higher axial diffusivity in major frontal bundles and temporal lobe fascicles (Piantoni *et al.*, 2013). This was found in fifteen young, healthy adult males with little variability in their white matter characteristics. In the present study, we failed to replicate these findings in our healthy control group. Factors explaining the discrepancy between studies could be sex difference in the control groups (77% males in the present study vs. 100% males in the study by Piantoni et al.), the age difference in the control groups (30.3 ± 13.4 years vs 25.4 ± 4.8 years, respectively), and the age-correction applied to our analyses. However, further studies with larger sample of healthy control subjects are necessary to clearly identify the association between individual differences in healthy white matter and slow wave characteristics.

Slow waves' morphology has also been studied in aging. Older adults showed a decline in slow wave amplitude and slope (Carrier *et al.*, 2011). These modifications in slow wave characteristics could be linked with the white matter loss observed with advancing age (Peters, 2002; Yap *et al.*, 2013) and were found to be associated with the thinning of specific cortical regions (Dube *et al.*, 2015).

By opposition with these previous studies in healthy young and older adults, our patients with widespread white matter damage had higher slow wave amplitudes and steeper slopes. Although we may have expected to see changes mirroring those seen in aging individuals, due to the documented loss of white matter in the aging brain, we did not find such results. Our results combined with these previous observations raises the possibility that the relationship between sleep slow waves and white matter structure is neither linear nor simple. To understand the association between white matter loss and slow waves observed in our TBI participants, we may refer to studies on partial cortical deafferentation. *In vivo* cat experiments in which a portion of the cortex is undercut have been performed to study the mechanisms of trauma-induced epilepsy (Avramescu and Timofeev, 2008; Avramescu *et al.*, 2009; Timofeev *et al.*, 2013). In these studies, the authors recorded enhanced slow-wave activity in the undercut hemisphere up to 16 weeks after the injury (Timofeev *et al.*, 2013). They hypothesized that this increased synchrony was caused by the increased network excitability observed chronically after partial deafferentation. Indeed, homeostatic plasticity in the brain works to maintain network excitability through changes in the balance of excitatory and inhibitory synapses and regulation of intrinsic neuronal excitability (Turrigiano *et al.*, 1998; Turrigiano, 2011). After partial deafferentation, network activity is acutely decreased, which engages upregulatory mechanisms to increase cortical excitability (Avramescu and Timofeev, 2008; Avramescu *et al.*, 2009). This concept is evidenced by another study in which they showed an acute reduction of slow-wave activity power in partially deafferentated cats, followed by a time-dependent recovery of slow-wave activity along with cortical excitability (Lemieux *et al.*, 2014). Although the models used in these studies are more crippling than what is observed in human TBI, these observations may partly explain the association we observed between white matter and NREM sleep slow waves in the present study. Diffuse white matter damage may acutely engage these homeostatic mechanisms to upregulate network excitability in the long term and cause part of the increase in neuronal synchrony we described. One study in humans has investigated cortical excitability changes after mild to moderate TBI (Nardone *et al.*, 2011). They found that a subset of patients, more specifically those with excessive daytime sleepiness, presented patterns of motor cortex hypoexcitability when compared to controls. However, the large majority of patients showed no such hypoexcitability. These measures were also

taken during wakefulness and on patients with minor brain damage only three months following the TBI. As such, this question remains open until more comprehensive experiments are performed.

On the other hand, it may also be that physical disconnection by diffuse white matter damage in TBI brings the cortex closer to its default state. Many argue that the default emergent activity patterns of the cortical network are highly synchronous slow waves (Sanchez-Vives *et al.*, 2017). Indeed, spontaneous slow waves emerge in states where the cortex is either physically or functionally disconnected from outside stimulation, such as deep sleep (Steriade *et al.*, 2001), anesthesia (Chauvette *et al.*, 2011), or *in-vitro* cortex slices (Sanchez-Vives and McCormick, 2000). Thalamo-cortical connections are especially vulnerable to TBI in humans, effectively bringing the cortex slightly closer to an isolated state. This may as well play a role in the large slow waves we observed in patients with important white matter damage.

Finally, we cannot exclude that this association between white matter damage and slow wave characteristics be due to the homeostatic sleep pressure (Borbely, 1982; Borbely and Achermann, 1999). An increase in slow-wave activity power at the beginning of the sleep period is the standard physiological marker of homeostatic sleep pressure (Borbely, 1982). Our TBI subjects with more severe white matter damage had higher slow-wave activity for all sleep cycles. Furthermore, steeper slow oscillation slopes and higher amplitude, the pattern observed in our TBI participants who had more white matter damage, were previously associated with a rise in homeostatic sleep pressure (Riedner et al., 2007; Vyazovskiy et al., 2007; Bersagliere and Achermann, 2010; Vyazovskiy et al., 2011; Rodriguez et al., 2016). Chronic white matter damage may cause TBI patients to accumulate need for sleep faster. Indeed, white matter damage due to TBI has very consistently been associated with impaired cognition (Kraus *et al.*, 2007; Kumar *et al.*, 2009; Palacios *et al.*, 2013; Spitz *et al.*, 2013; Arenth *et al.*, 2014; Kim *et al.*, 2014), and TBI patients have been shown to exert more mental effort for the same task than healthy subjects (Belmont *et al.*, 2009). A study using fMRI has also observed that while performing a cognitive task, TBI patients have increased brain activity compared to healthy subjects in several brain regions

519 believed to be involved in mental fatigue, which is thought to represent higher mental effort
520 (Kohl *et al.*, 2009). In the present study, we found that TBI patients with more white matter
521 damage also had more severe subjective fatigue. Similar results were observed in other
522 studies (Clark *et al.*, 2017 ;Schonberger *et al.*, 2017). Taken together, these findings suggest
523 that chronic white matter damage causes TBI patients to accumulate mental fatigue faster
524 during the day, which may increase homeostatic sleep pressure and enhances sleep
525 synchrony during subsequent sleep. A valid concern would be that these patients were under
526 sleep deprivation, causing the aforementioned phenomena. However, as mentioned
527 previously all patients completed daily sleep agendas and wore an activity monitor device
528 the week preceding testing, all of which confirm that these patients had similar total sleep
529 time when compared with controls. Still, protocols specifically assessing the evolution of
530 fatigue throughout the day in relation with sleep homeostatic pressure need to be performed
531 to adequately verify this hypothesis.
532
533 ***Conclusion***
534 This study represents the first to explore the association between sleep slow waves and
535 white matter structure in adults with white matter damage. Our results showed strong
536 associations between white matter and slow waves occurring during NREM sleep. More
537 damaged brains were associated with markers of higher brain synchrony during sleep, and
538 these associations could be caused by cerebral disconnection or by elevated homeostatic
539 sleep pressure in TBI patients. White matter damage does not seem to impede the
540 restorative function of sleep as we first thought. These results bring new insight to
541 understand the pathophysiology of sleep disturbances and fatigue observed after TBI as well
542 as factors influencing brain synchrony during sleep. Moreover, this study challenges the
543 current hypotheses regarding the role of white matter structure on the brain ability to
544 synchronize its cortical regions during sleep and produce restorative sleep.
545

546 ## Acknowledgements

547 For their support in data acquisition, the authors wish to thank Catherine Duclos, Solenne
548 Van der Maren, Caroline D'Aragon, Julien Lauzier, Carollyn Hurst, and André Cyr.

Funding

This study was funded by government granting agencies by grants to NG as a principal investigator: Canadian Institutes of Health Research (CIHR) and Fonds de Recherche Santé-Québec (FRQS). ES and AAB received scholarships from the CIHR and FRQS. NG received a salary award from the FRQS. JC received a salary award from the CIHR. MD holds a Université de Sherbrooke Research Chair in Neuroinformatics.

Author contributions

ES and NG participated in study conception and design. ES, HEK, CA, HB, and DG participated in data acquisition. ES, CB, and KM participated in data analysis. ES, AAB, MD, JC, and NG participated in data interpretation. ES wrote the manuscript. NG assisted in writing the manuscript. All authors critically revised the manuscript and approved the final version.

Competing interests

The authors declare no competing interests.

References

Aeschbach D, Borbely AA. All-night dynamics of the human sleep EEG. Journal of sleep research 1993; 2(2): 70-81.

Arenth PM, Russell KC, Scanlon JM, Kessler LJ, Ricker JH. Corpus callosum integrity and neuropsychological performance after traumatic brain injury: a diffusion tensor imaging study. The Journal of head trauma rehabilitation 2014; 29(2): E1-e10.

Avramescu S, Nita DA, Timofeev I. Neocortical post-traumatic epileptogenesis is associated with loss of GABAergic neurons. Journal of neurotrauma 2009; 26(5): 799-812.

Avramescu S, Timofeev I. Synaptic strength modulation after cortical trauma: a role in epileptogenesis. The Journal of neuroscience : the official journal of the Society for Neuroscience 2008; 28(27): 6760-72.

Beck AT, Epstein N, Brown G, Steer RA. An inventory for measuring clinical anxiety: psychometric properties. Journal of consulting and clinical psychology 1988; 56(6): 893.

Beck AT, Steer RA, Brown GK. Beck depression inventory-II. San Antonio 1996; 78(2): 490-8.

583 Belmont A, Agar N, Azouvi P. Subjective fatigue, mental effort, and attention deficits after
584 severe traumatic brain injury. Neurorehabilitation and neural repair 2009; 23(9): 939-44.
585 Benson RR, Meda SA, Vasudevan S, Kou Z, Govindarajan KA, Hanks RA*, et al.* Global white
586 matter analysis of diffusion tensor images is predictive of injury severity in traumatic brain
587 injury. Journal of neurotrauma 2007; 24(3): 446-59.
588 Bersagliere A, Achermann P. Slow oscillations in human non-rapid eye movement sleep
589 electroencephalogram: effects of increased sleep pressure. Journal of sleep research 2010;
590 19(1 Pt 2): 228-37.
591 Borbely AA. A two process model of sleep regulation. Human neurobiology 1982; 1(3): 195-
592 204.
593 Borbely AA, Achermann P. Sleep homeostasis and models of sleep regulation. Journal of
594 biological rhythms 1999; 14(6): 557-68.
595 Buchmann A, Kurth S, Ringli M, Geiger A, Jenni OG, Huber R. Anatomical markers of sleep
596 slow wave activity derived from structural magnetic resonance images. Journal of sleep
597 research 2011; 20(4): 506-13.
598 Buysse DJ, Reynolds CF, 3rd, Monk TH, Berman SR, Kupfer DJ. The Pittsburgh Sleep Quality
599 Index: a new instrument for psychiatric practice and research. Psychiatry research 1989;
600 28(2): 193-213.
601 Carrier J, Viens I, Poirier G, Robillard R, Lafortune M, Vandewalle G*, et al.* Sleep slow wave
602 changes during the middle years of life. The European journal of neuroscience 2011; 33(4):
603 758-66.
604 Chauvette S, Crochet S, Volgushev M, Timofeev I. Properties of slow oscillation during slow-
605 wave sleep and anesthesia in cats. The Journal of neuroscience : the official journal of the
606 Society for Neuroscience 2011; 31(42): 14998-5008.
607 Clark AL, Delano-Wood L, Sorg SF, Werhane ML, Hanson KL, Schiehser DM. Cognitive fatigue
608 is associated with reduced anterior internal capsule integrity in veterans with history of mild
609 to moderate traumatic brain injury. Brain imaging and behavior 2017; 11(5): 1548-54.
610 Crunelli V, David F, Lorincz ML, Hughes SW. The thalamocortical network as a single slow
611 wave-generating unit. Current opinion in neurobiology 2015; 31: 72-80.
612 Diekelmann S, Born J. The memory function of sleep. Nature reviews Neuroscience 2010;
613 11(2): 114-26.
614 Dube J, Lafortune M, Bedetti C, Bouchard M, Gagnon JF, Doyon J*, et al.* Cortical thinning
615 explains changes in sleep slow waves during adulthood. The Journal of neuroscience : the
616 official journal of the Society for Neuroscience 2015; 35(20): 7795-807.
617 Duclos C, Dumont M, Wiseman-Hakes C, Arbour C, Mongrain V, Gaudreault PO*, et al.* Sleep
618 and wake disturbances following traumatic brain injury. Pathologie-biologie 2014; 62(5):
619 252-61.
620 Haberg AK, Olsen A, Moen KG, Schirmer-Mikalsen K, Visser E, Finnanger TG*, et al.* White
621 matter microstructure in chronic moderate-to-severe traumatic brain injury: Impact of
622 acute-phase injury-related variables and associations with outcome measures. Journal of
623 neuroscience research 2015; 93(7): 1109-26.
624 Johns MW. A new method for measuring daytime sleepiness: the Epworth sleepiness scale.
625 Sleep 1991; 14(6): 540-5.
626 Kennedy MR, Wozniak JR, Muetzel RL, Mueller BA, Chiou HH, Pantekoek K*, et al.* White matter
627 and neurocognitive changes in adults with chronic traumatic brain injury. Journal of the
628 International Neuropsychological Society : JINS 2009; 15(1): 130-6.

629 Kim J, Parker D, Whyte J, Hart T, Pluta J, Ingalhalikar M*, et al.* Disrupted structural
630 connectome is associated with both psychometric and real-world neuropsychological
631 impairment in diffuse traumatic brain injury. Journal of the International
632 Neuropsychological Society : JINS 2014; 20(9): 887-96.
633 Kinnunen KM, Greenwood R, Powell JH, Leech R, Hawkins PC, Bonnelle V*, et al.* White matter
634 damage and cognitive impairment after traumatic brain injury. Brain : a journal of neurology
635 2011; 134(Pt 2): 449-63.
636 Kohl AD, Wylie GR, Genova HM, Hillary FG, Deluca J. The neural correlates of cognitive fatigue
637 in traumatic brain injury using functional MRI. Brain injury 2009; 23(5): 420-32.
638 Kraus MF, Susmaras T, Caughlin BP, Walker CJ, Sweeney JA, Little DM. White matter integrity
639 and cognition in chronic traumatic brain injury: a diffusion tensor imaging study. Brain : a
640 journal of neurology 2007; 130(Pt 10): 2508-19.
641 Krupp LB, LaRocca NG, Muir-Nash J, Steinberg AD. The fatigue severity scale. Application to
642 patients with multiple sclerosis and systemic lupus erythematosus. Archives of neurology
643 1989; 46(10): 1121-3.
644 Kumar R, Husain M, Gupta RK, Hasan KM, Haris M, Agarwal AK*, et al.* Serial changes in the
645 white matter diffusion tensor imaging metrics in moderate traumatic brain injury and
646 correlation with neuro-cognitive function. Journal of neurotrauma 2009; 26(4): 481-95.
647 Lemieux M, Chen JY, Lonjers P, Bazhenov M, Timofeev I. The impact of cortical
648 deafferentation on the neocortical slow oscillation. The Journal of neuroscience : the official
649 journal of the Society for Neuroscience 2014; 34(16): 5689-703.
650 Mander BA, Marks SM, Vogel JW, Rao V, Lu B, Saletin JM*, et al.* beta-amyloid disrupts human
651 NREM slow waves and related hippocampus-dependent memory consolidation. Nature
652 neuroscience 2015; 18(7): 1051-7.
653 Marshall L, Helgadottir H, Molle M, Born J. Boosting slow oscillations during sleep potentiates
654 memory. Nature 2006; 444(7119): 610-3.
655 Massimini M, Huber R, Ferrarelli F, Hill S, Tononi G. The sleep slow oscillation as a traveling
656 wave. The Journal of neuroscience : the official journal of the Society for Neuroscience 2004;
657 24(31): 6862-70.
658 Menon DK, Schwab K, Wright DW, Maas AI. Position statement: definition of traumatic brain
659 injury. Archives of physical medicine and rehabilitation 2010; 91(11): 1637-40.
660 Morawska MM, Buchele F, Moreira CG, Imbach LL, Noain D, Baumann CR. Sleep Modulation
661 Alleviates Axonal Damage and Cognitive Decline after Rodent Traumatic Brain Injury. The
662 Journal of neuroscience : the official journal of the Society for Neuroscience 2016; 36(12):
663 3422-9.
664 Mori S, Oishi K, Jiang H, Jiang L, Li X, Akhter K*, et al.* Stereotaxic white matter atlas based on
665 diffusion tensor imaging in an ICBM template. NeuroImage 2008; 40(2): 570-82.
666 Murphy M, Riedner BA, Huber R, Massimini M, Ferrarelli F, Tononi G. Source modeling sleep
667 slow waves. Proceedings of the National Academy of Sciences of the United States of America
668 2009; 106(5): 1608-13.
669 Nardone R, Bergmann J, Kunz A, Caleri F, Seidl M, Tezzon F*, et al.* Cortical excitability changes
670 in patients with sleep-wake disturbances after traumatic brain injury. Journal of
671 neurotrauma 2011; 28(7): 1165-71.
672 Ouellet MC, Beaulieu-Bonneau S, Morin CM. Sleep-wake disturbances after traumatic brain
673 injury. The Lancet Neurology 2015; 14(7): 746-57.

674 Palacios EM, Sala-Llonch R, Junque C, Roig T, Tormos JM, Bargallo N*, et al.* White matter/gray
675 matter contrast changes in chronic and diffuse traumatic brain injury. Journal of
676 neurotrauma 2013; 30(23): 1991-4.
677 Peters A. Structural changes in the normally aging cerebral cortex of primates. Progress in
678 brain research 2002; 136: 455-65.
679 Piantoni G, Poil SS, Linkenkaer-Hansen K, Verweij IM, Ramautar JR, Van Someren EJ*, et al.*
680 Individual differences in white matter diffusion affect sleep oscillations. The Journal of
681 neuroscience : the official journal of the Society for Neuroscience 2013; 33(1): 227-33.
682 Pitkonen M, Abo-Ramadan U, Marinkovic I, Pedrono E, Hasan KM, Strbian D*, et al.* Long-term
683 evolution of diffusion tensor indices after temporary experimental ischemic stroke in rats.
684 Brain research 2012; 1445: 103-10.
685 Riedner BA, Vyazovskiy VV, Huber R, Massimini M, Esser S, Murphy M*, et al.* Sleep
686 homeostasis and cortical synchronization: III. A high-density EEG study of sleep slow waves
687 in humans. Sleep 2007; 30(12): 1643-57.
688 Rodriguez AV, Funk CM, Vyazovskiy VV, Nir Y, Tononi G, Cirelli C. Why Does Sleep Slow-Wave
689 Activity Increase After Extended Wake? Assessing the Effects of Increased Cortical Firing
690 During Wake and Sleep. The Journal of neuroscience : the official journal of the Society for
691 Neuroscience 2016; 36(49): 12436-47.
692 Sanchez-Vives MV, Massimini M, Mattia M. Shaping the Default Activity Pattern of the Cortical
693 Network. Neuron 2017; 94(5): 993-1001.
694 Sanchez-Vives MV, McCormick DA. Cellular and network mechanisms of rhythmic recurrent
695 activity in neocortex. Nature neuroscience 2000; 3(10): 1027-34.
696 Schonberger M, Reutens D, Beare R, O'Sullivan R, Rajaratnam SMW, Ponsford J. Brain lesion
697 correlates of fatigue in individuals with traumatic brain injury. Neuropsychological
698 rehabilitation 2017; 27(7): 1056-70.
699 Smith SM, Jenkinson M, Johansen-Berg H, Rueckert D, Nichols TE, Mackay CE*, et al.* Tract-
700 based spatial statistics: voxelwise analysis of multi-subject diffusion data. NeuroImage 2006;
701 31(4): 1487-505.
702 Smith SM, Jenkinson M, Woolrich MW, Beckmann CF, Behrens TE, Johansen-Berg H*, et al.*
703 Advances in functional and structural MR image analysis and implementation as FSL.
704 NeuroImage 2004; 23 Suppl 1: S208-19.
705 Smith SM, Nichols TE. Threshold-free cluster enhancement: addressing problems of
706 smoothing, threshold dependence and localisation in cluster inference. NeuroImage 2009;
707 44(1): 83-98.
708 Spitz G, Maller JJ, O'Sullivan R, Ponsford JL. White matter integrity following traumatic brain
709 injury: the association with severity of injury and cognitive functioning. Brain topography
710 2013; 26(4): 648-60.
711 Steriade M. Grouping of brain rhythms in corticothalamic systems. Neuroscience 2006;
712 137(4): 1087-106.
713 Steriade M, Timofeev I, Grenier F. Natural waking and sleep states: a view from inside
714 neocortical neurons. Journal of neurophysiology 2001; 85(5): 1969-85.
715 Teasdale G, Jennett B. Assessment of coma and impaired consciousness. A practical scale.
716 Lancet (London, England) 1974; 2(7872): 81-4.
717 Timofeev I, Sejnowski TJ, Bazhenov M, Chauvette S, Grand LB. Age dependency of trauma-
718 induced neocortical epileptogenesis. Frontiers in cellular neuroscience 2013; 7: 154.

719 Tononi G, Cirelli C. Sleep function and synaptic homeostasis. Sleep medicine reviews 2006;
720 10(1): 49-62.
721 Turrigiano G. Too many cooks? Intrinsic and synaptic homeostatic mechanisms in cortical
722 circuit refinement. Annual review of neuroscience 2011; 34: 89-103.
723 Turrigiano GG, Leslie KR, Desai NS, Rutherford LC, Nelson SB. Activity-dependent scaling of
724 quantal amplitude in neocortical neurons. Nature 1998; 391(6670): 892-6.
725 Vyazovskiy VV, Cirelli C, Tononi G. Electrophysiological correlates of sleep homeostasis in
726 freely behaving rats. Progress in brain research 2011; 193: 17-38.
727 Vyazovskiy VV, Riedner BA, Cirelli C, Tononi G. Sleep homeostasis and cortical
728 synchronization: II. A local field potential study of sleep slow waves in the rat. Sleep 2007;
729 30(12): 1631-42.
730 Winkler AM, Ridgway GR, Webster MA, Smith SM, Nichols TE. Permutation inference for the
731 general linear model. NeuroImage 2014; 92: 381-97.
732 Xie L, Kang H, Xu Q, Chen MJ, Liao Y, Thiyagarajan M, *et al.* Sleep drives metabolite clearance
733 from the adult brain. Science (New York, NY) 2013; 342(6156): 373-7.
734 Yap QJ, Teh I, Fusar-Poli P, Sum MY, Kuswanto C, Sim K. Tracking cerebral white matter
735 changes across the lifespan: insights from diffusion tensor imaging studies. Journal of neural
736 transmission (Vienna, Austria : 1996) 2013; 120(9): 1369-95.
737

TABLE 1. Demographic characteristics, questionnaires, neuropsychological assessment and sleep macro-architecture

	TBI (n = 23)	Controls (n= 27)	*t*-value (*p*-value)
Age (years)	30.5 (11.1)	30.3 (13.4)	0.1 (0.95)
Sex (nb. of male/female)	17/6	21/6	0.3 (0.75)
Education (years)	13.0 (3.3)	15.2 (2.1)	**2.9 (0.006)**
GCS at hospital admission	8.5 (3.3)	-	-
Length of posttraumatic amnesia (days)	17.0 (17.6)	-	-
Time after injury (months)	23.4 (9.4)	-	-
Return to work/school (%)	60	-	-
Questionnaires			
Fatigue Severity Scale	40.1 (16.1)	30.7 (11.1)	**2.4 (0.02)**
Epworth Sleepiness Scale	8.4 (5.7)	6.5 (4.1)	1.3 (0.19)
Pittsburgh Sleep Quality Index	6.7 (3.2)	4.2 (2.5)	**2.9 (0.005)**
Beck Anxiety Inventory	9.3 (10.0)	4.6 (6.3)	**2.1 (0.04)**
Beck Depression Inventory II	17.4 (10.7)	4.9 (6.0)	**5.2 (<0.001)**
Neuropsychological assessment			
Trail Making Test A time (sec)	30.8 (13.1)	25.6 (9.2)	1.6 (0.13)
Trail Making Test B time (sec)	84.0 (35.0)	63.8 (26.3)	**2.2 (0.03)**
Color-Word interference 1 time (sec)	31.6 (6.1)	27.4 (4.6)	**2.6 (0.01)**
Color-Word interference 2 time (sec)	24.0 (4.8)	19.1 (3.2)	**4.1 (<0.001)**

Color-Word interference 3 time (sec)	60.0 (13.4)	50.0 (12.6)	**2.7 (0.01)**
Color-Word interference 4 time (sec)	68.5 (19.7)	50.3 (8.3)	**4.3 (<0.001)**
Hopkins Verbal Learning Test (total learning)	23.6 (5.3)	26.1 (3.7)	1.9 (0.07)
Sleep macro-architecture on PSG			
Sleep latency (min)	16.1 (16.7)	20.3 (29.1)	0.6 (0.53)
REM sleep latency (min)	106.0 (90.7)	114.1 (62.6)	0.4 (0.72)
Total sleep time (min)	465.7 (59.4)	441.0 (59.5)	1.5 (0.15)
Number of awakenings	33.8 (13.3)	27.8 (10.8)	1.7 (0.09)
Wake after sleep onset (min)	57.8 (46.1)	48.0 (33.7)	0.8 (0.41)
Apnea-hypopnea index (events/hour)	2.6 (3.5)	2.2 (2.5)	0.5 (0.63)
Sleep efficiency (%)	88.6 (9.7)	90.2 (6.8)	0.7 (0.52)
Stage N1 sleep (%)	11.7 (6.2)	10.5 (5.2)	0.7 (0.48)
Stage N2 sleep (%)	53.7 (7.1)	52.5 (6.4)	0.6 (0.53)
Stage N3 sleep (%)	16.4 (9.7)	17.9 (8.9)	0.6 (0.56)
REM sleep (%)	18.3 (4.4)	19.1 (5.4)	0.6 (0.55)

Data are presented as mean (standard deviation), when applicable. TBI: Traumatic brain injury, GCS: Glasgow Coma Scale, PSG: Polysomnography, REM: Rapid eye movement

TABLE 2. Results of the Group X Electrode cluster ANOVAs on slow wave characteristics

	TBI (n = 23)		Controls (n = 27)		Main group effect
	Frontal cluster	Central cluster	Frontal cluster	Central cluster	
Peak-to-peak amplitude (µV)	130.7 (13.4)	122.4 (13.4)	135.7 (20.1)	123.0 (16.7)	$F = 1.2$; $P = 0.28$
Negative duration (s)	0.487 (0.048)	0.478 (0.047)	0.456 (0.040)	0.457 (0.049)	$F = 4.0$; $P = 0.05$
Positive duration (s)	0.538 (0.052)	0.531 (0.056)	0.500 (0.051)	0.497 (0.054)	**$F = 8.0$; $P < 0.01$**
Frequency (Hz)	1.09 (0.11)	1.12 (0.13)	1.17 (0.12)	1.20 (0.13)	**$F = 6.9$; $P = 0.01$**
N-to-P slope (µV/s)	340.9 (59.4)	315.0 (56.3)	380.2 (87.5)	339.7 (74.8)	**$F = 4.8$; $P = 0.03$**
Density (nb./min)	9.0 (5.0)	7.0 (4.3)	10.3 (5.0)	7.9 (4.3)	$F = 1.4$; $P = 0.25$

No interaction or cluster effects were observed. Data are presented as mean (standard deviation). TBI: Traumatic brain injury, N-to-P: Negative to positive

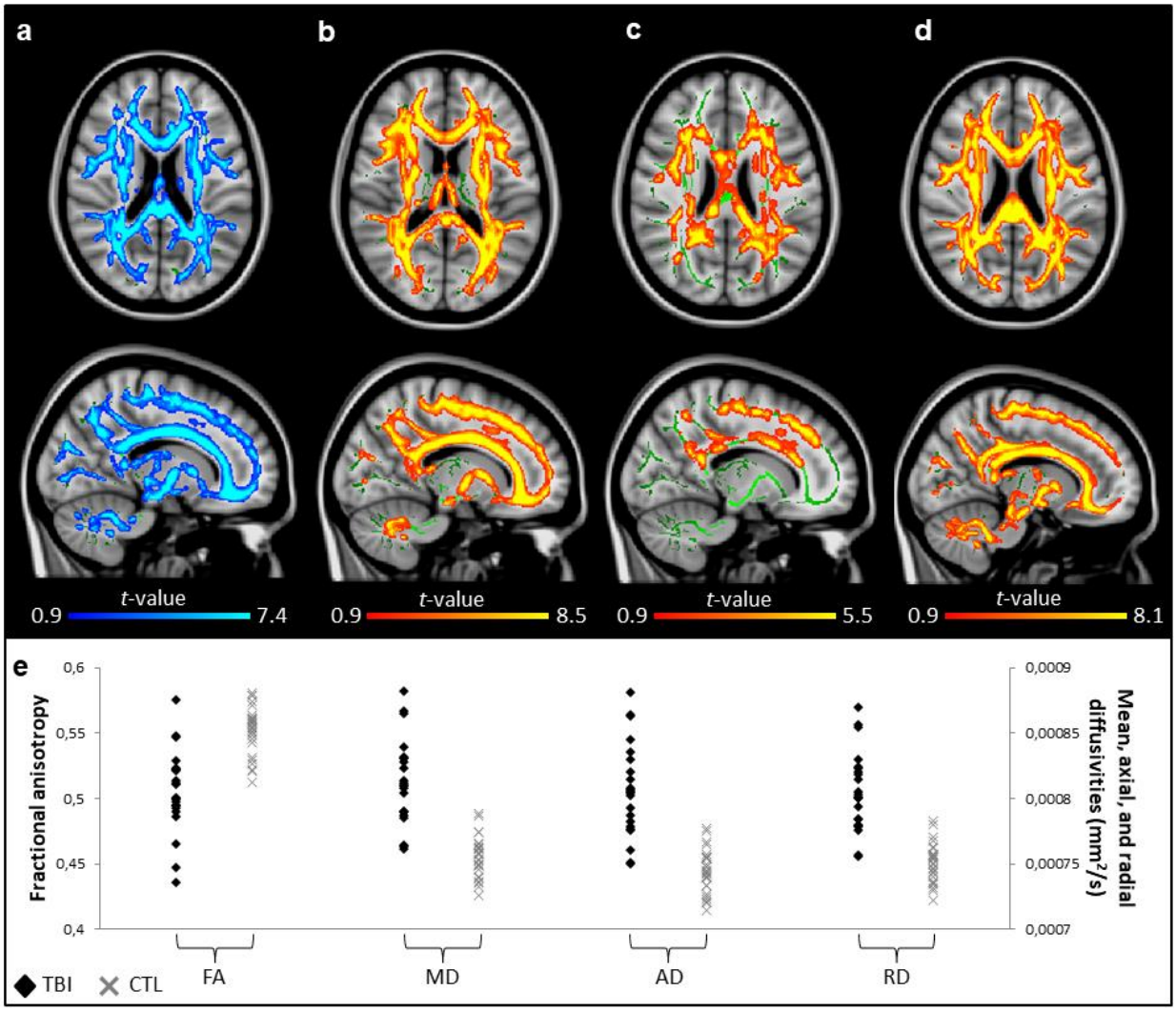

FIGURE 1. Group differences on diffusion metrics. TBSS voxel-wise contrasts between traumatic brain injury (TBI) and control (CTL) groups (blue, TBI < CTL; red to yellow, TBI > CTL) for **(a)** fractional anisotropy (FA), **(b)** mean diffusivity (MD), **(c)** axial diffusivity (AD), and **(d)** radial diffusivity (RD). Significant results are overlaid over the MNI152 T1 1mm brain and the mean fractional anisotropy skeleton (in green). Significant increases in the TBI group compared to the Control group are shown in the red to yellow scale and significant decreases are shown in light blue. The mean value of all significant clusters is represented on the graph for each subject. Significant results were thresholded at $p<0.05$ controlled for age and corrected for multiple comparisons.

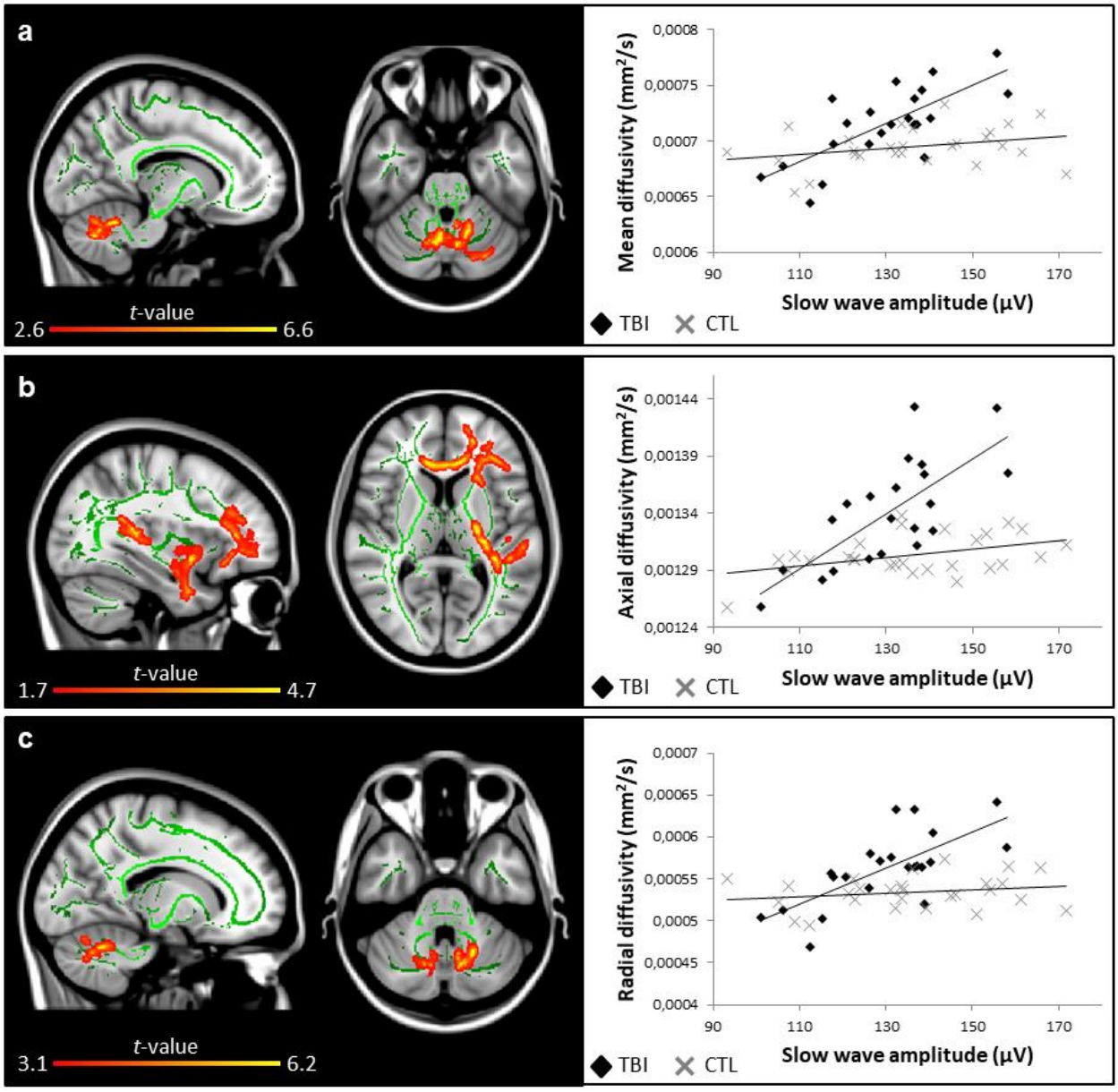

FIGURE 2. Slow wave amplitude and white matter damage. Areas in traumatic brain injury (TBI) group where slow wave amplitude is positively correlated (red to yellow colored areas) with **(a)** mean diffusivity (r = 0.81), **(b)** axial diffusivity (r = 0.74), and **(c)** radial diffusivity (r = 0.78). Significant results are overlaid over the MNI152 T1 1mm brain and the mean fractional anisotropy skeleton (in green). The correlation between the mean value of all significant clusters and slow wave amplitude is represented on the graphs. No area of negative correlation was found in the TBI group and no significant correlation was found for the control group. Results are thresholded at $p<0.05$, adjusted for age and corrected for multiple comparisons.

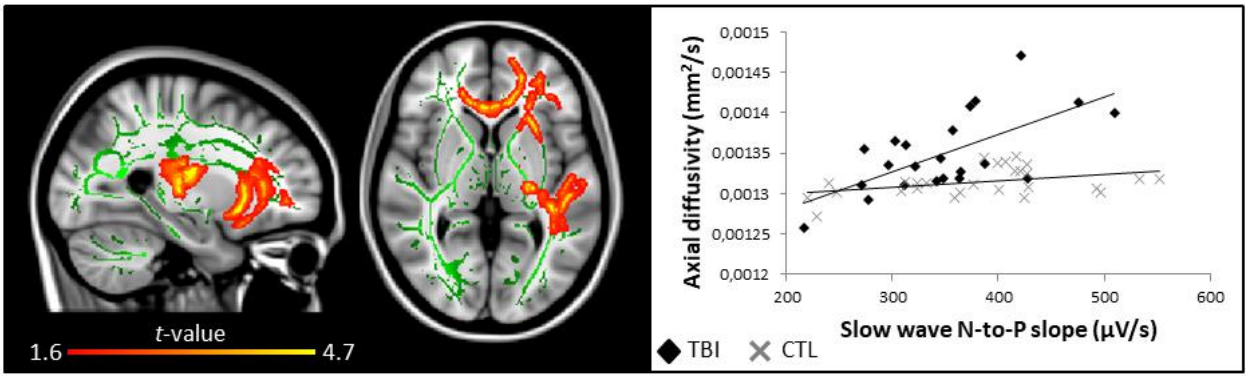

FIGURE 3. Slow wave slope and white matter damage. Areas in traumatic brain injury (TBI) group where slow wave negative-to-positive slope is correlated (red to yellow, positive correlation) with axial diffusivity (r = 0.64). Significant results are overlaid over the MNI152 T1 1mm brain and the mean fractional anisotropy skeleton (in green). The correlation between the mean value of all significant clusters and slow wave N-to-P slope is represented on the graph. No area of negative correlation was found in the TBI group and no significant correlation was found for the control group. Results are thresholded at $p<0.05$, adjusted for age and corrected for multiple comparisons.

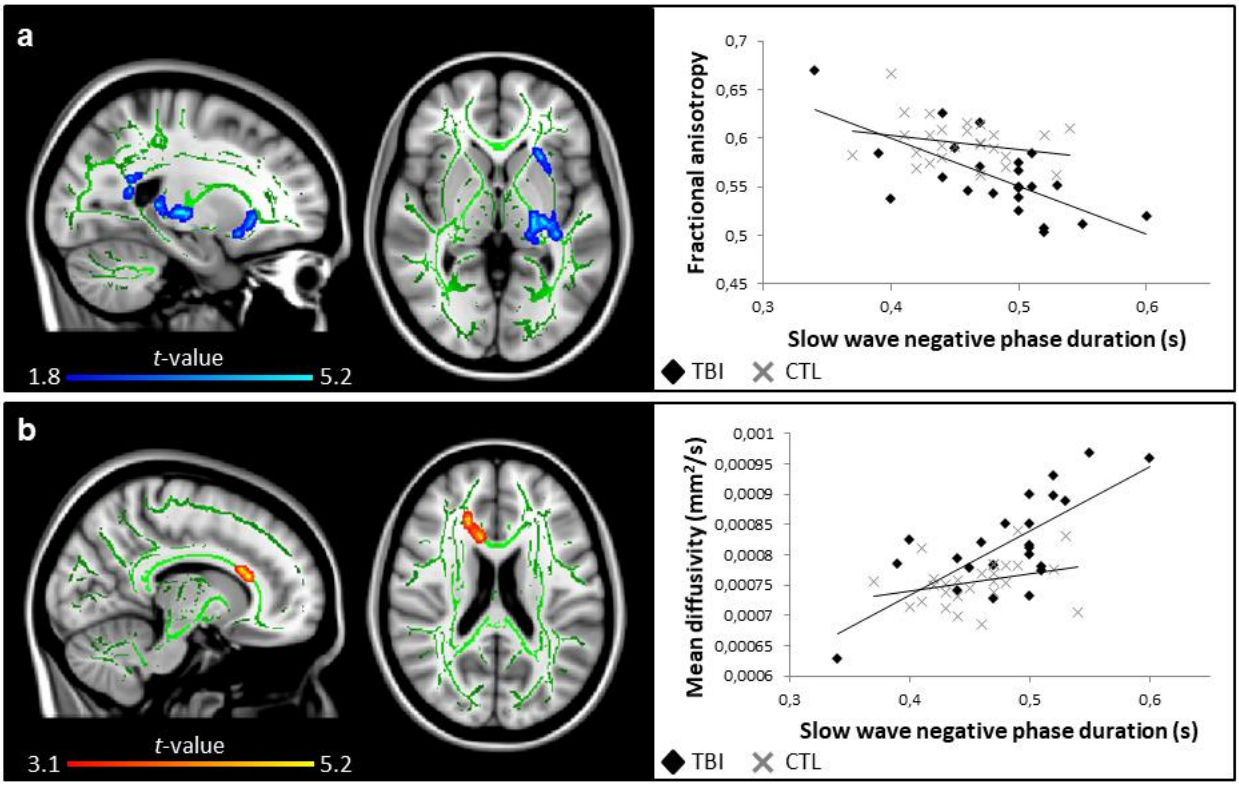

FIGURE 4. Slow wave negative phase duration and white matter damage. Areas in traumatic brain injury (TBI) group where slow wave negative phase duration is correlated (blue, negative correlation; red to yellow, positive correlation) with **(a)** fractional anisotropy (r = -0.69) and **(b)** mean diffusivity (r = 0.73). Significant results are overlaid over the MNI152 T1 1mm brain and the mean fractional anisotropy skeleton (in green). The correlation between the mean value of all significant clusters and slow wave negative phase duration is represented on the graphs. No significant correlation was found for the control group. Results are thresholded at $p<0.05$, adjusted for age and corrected for multiple comparisons.

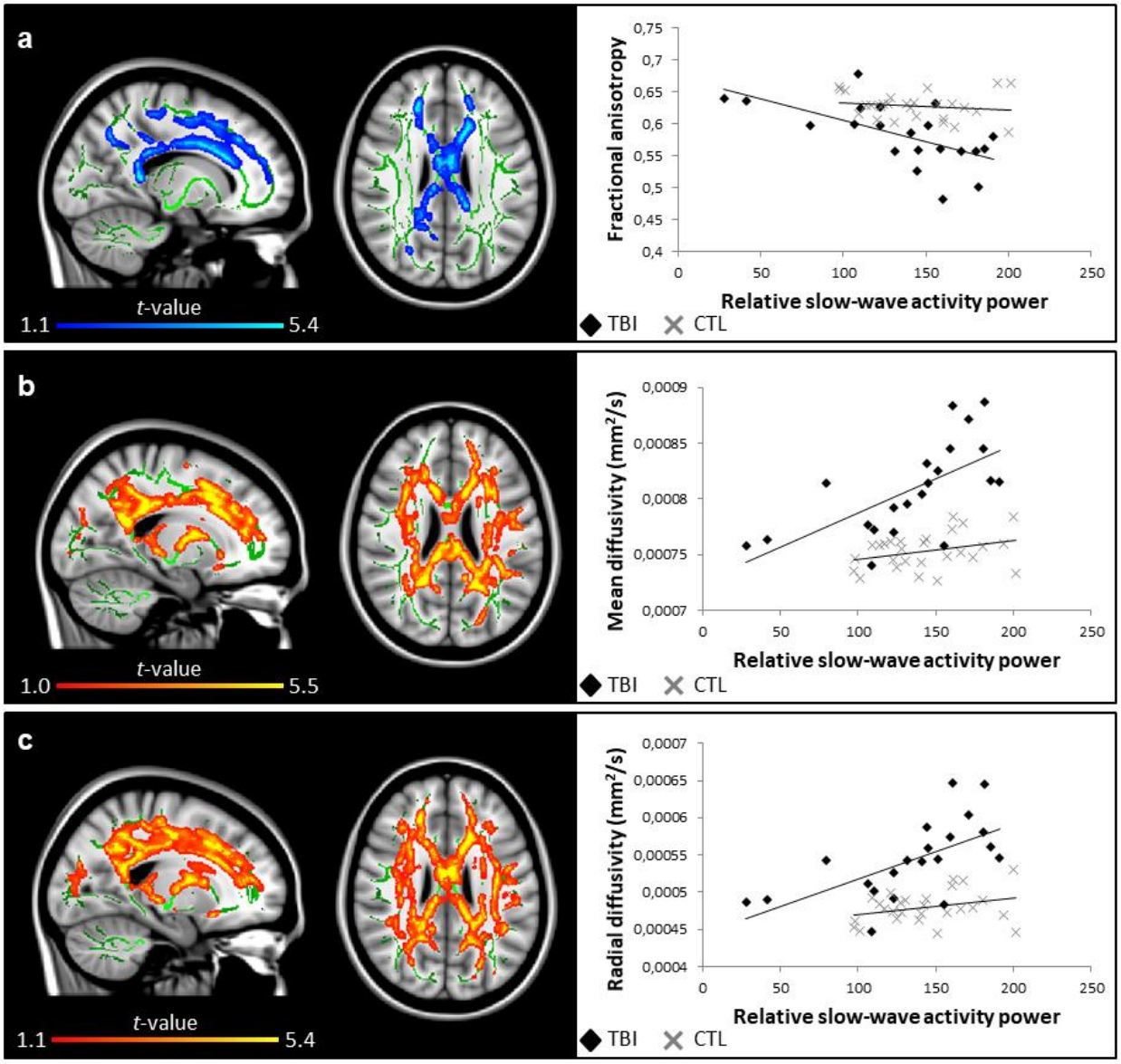

FIGURE 5. Relative slow-wave activity power in the 1st sleep cycle and white matter damage. Areas in traumatic brain injury (TBI) group where slow wave activity power is correlated (blue, negative correlation; red to yellow, positive correlation) with **(a)** fractional anisotropy (r = -0.63), **(b)** mean diffusivity (r = 0.70), and **(c)** radial diffusivity (r = 0.65). Significant results are overlaid over the MNI152 T1 1mm brain and the mean fractional anisotropy skeleton (in green). The correlation between the mean value of all significant clusters and relative slow-wave activity power is represented on the graphs. No significant correlation was found for the control group. Results are thresholded at $p<0.05$, adjusted for age and corrected for multiple comparisons.

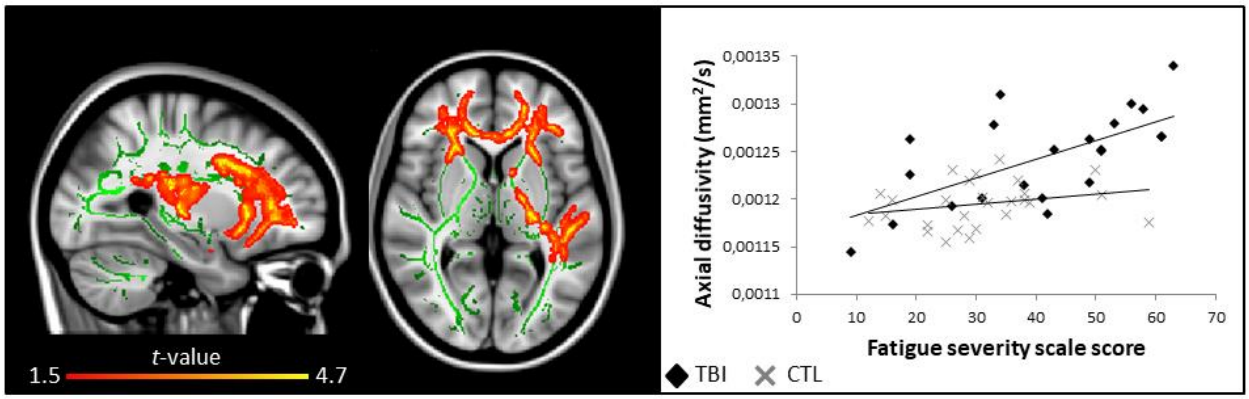

FIGURE 6. Self-reported fatigue and white matter damage. Areas in traumatic brain injury (TBI) group where fatigue is correlated (red to yellow, positive correlation) with axial diffusivity ($r = 0.66$). Significant results are overlaid over the MNI152 T1 1mm brain and the mean fractional anisotropy skeleton (in green). The correlation between the mean value of all significant clusters and fatigue is represented on the graph. No area of negative correlation was found in the TBI group, and no significant correlation was found for the control group. Results are thresholded at $p<0.05$, adjusted for age and corrected for multiple comparisons.

SUPPLEMENTARY TABLE I. Prescribed medication intake of participants with traumatic brain injury

Patient ID	Name of medication	Dose (mg)	Frequency of intake	Additional comments
1	Methyphenidate (Ritalin®)	20	2 / day	Ceased Ritalin 3 days before testing
	Escitalopram (Cipralex®)	20	2 / day	
	Quetiapine (Seroquel®)	25	1 / day	
	Ibuprofen (Advil®)	200	3 / day	
2	Methyphenidate (Concerta®)	27	1 / day	Ceased all 7 days before testing
	Methyphenidate (Concerta®)	18	1 / day	
3	Venlafaxine (Effexor®)	37.5	1 / day	
	Trazodone (Apo-Trazodone®)	50	2 / day	
	Methyphenidate (Concerta®)	36	2 / day	
4	Venlafaxine (Effexor®)	75	1 / day	
5	Divalproex (Epival®)	500	2 / day	
6	Methyphenidate (Concerta®)	54	1 / day	
7	Amitriptyline (Elavil®)	15	1 / day	Ceased all 3 days before testing
	Ibuprofen (Advil®)	200	1 / day	
8	Lisdexamfetamine (Vyvance®)	60	1 / day	Ceased all 4 days before testing

Participants with no medication intake are not represented in this table

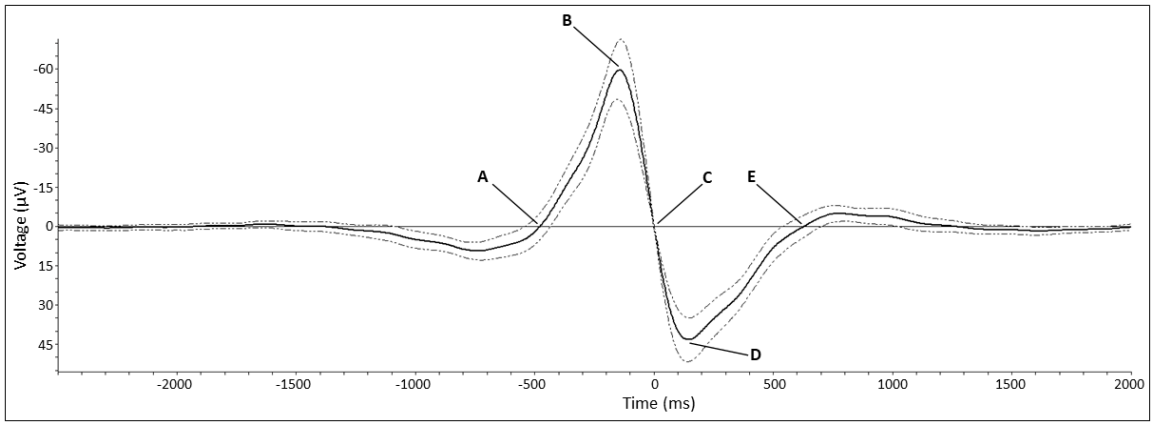

SUPPLEMENTARY FIGURE 1. Representative morphological characteristics of a slow wave. This slow wave represents the average (and standard deviation, in dotted lines) of every individual slow wave detected for all 27 healthy controls on selected frontal and central derivations (F3, F4, Fz, C3, C4, Cz). The detection occurred during the NREM N2 and N3 sleep stages for all sleep cycles of the night. The following characteristics can be seen on this figure: peak-to-peak amplitude (voltage difference from B to D), frequency (oscillation speed), negative-to-positive slope (slope from B to D), negative phase duration (time from A to C), and positive phase duration (time from C to E).

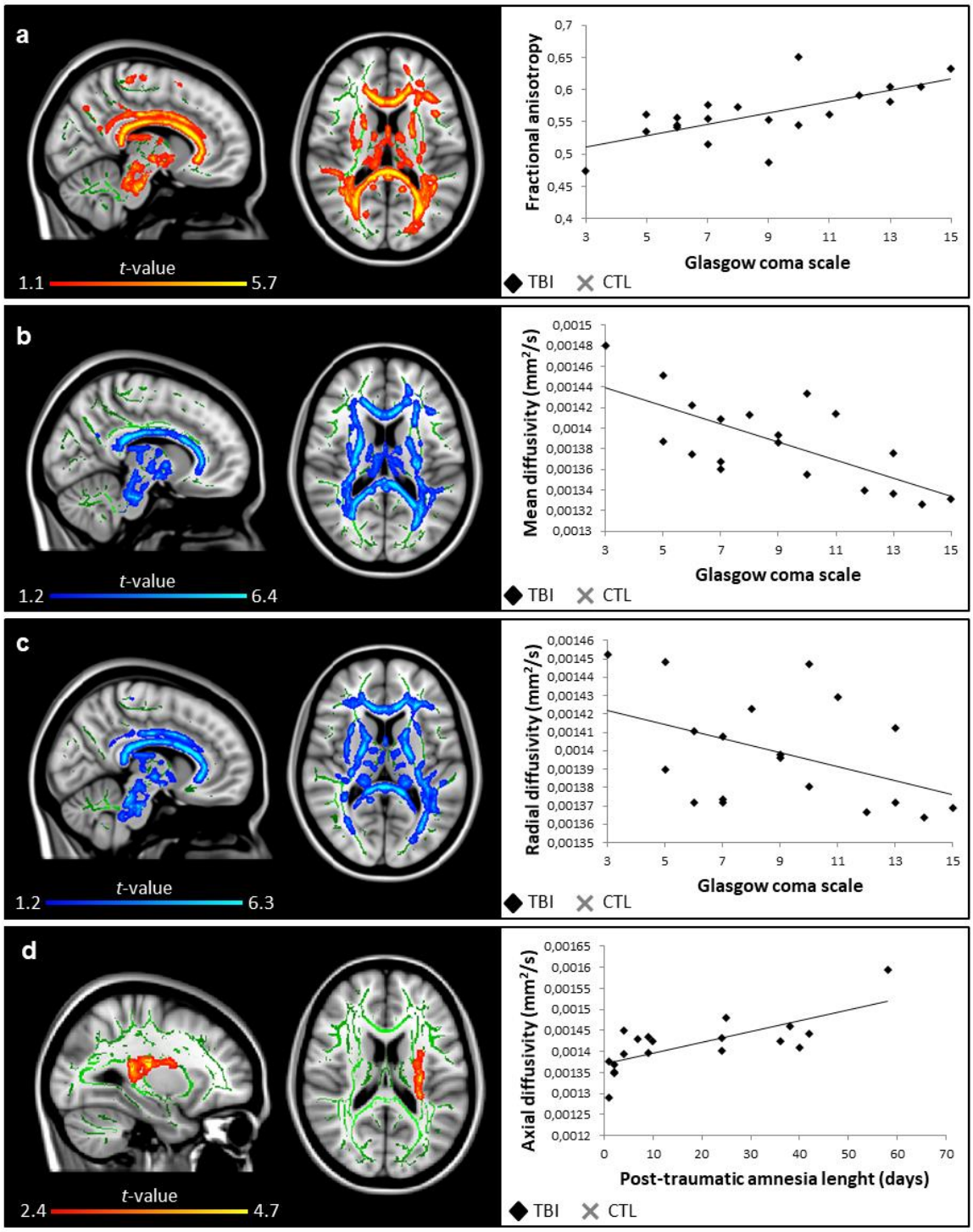

SUPPLEMENTARY FIGURE 2. Markers of traumatic brain injury severity and white matter damage. Areas in traumatic brain injury (TBI) group where markers of severity are correlated (blue, negative correlation; red to yellow, positive correlation) with **(a)** fractional anisotropy (r = 0.77), **(b)** mean diffusivity (r = -0.93), **(c)** radial diffusivity (r = -0.77), and **(d)** axial diffusivity (r = 0.83). Significant results are overlaid over the MNI152 T1 1mm brain and the mean fractional anisotropy skeleton (in green). The correlation

between the mean value of all significant clusters and markers of severity is represented on the graphs. A lower score on the Glasgow coma scale and a lengthier period of post-traumatic amnesia represent a more severe TBI. No significant correlation was found for the control group. Results are thresholded at p<0.05, adjusted for age and corrected for multiple comparisons.

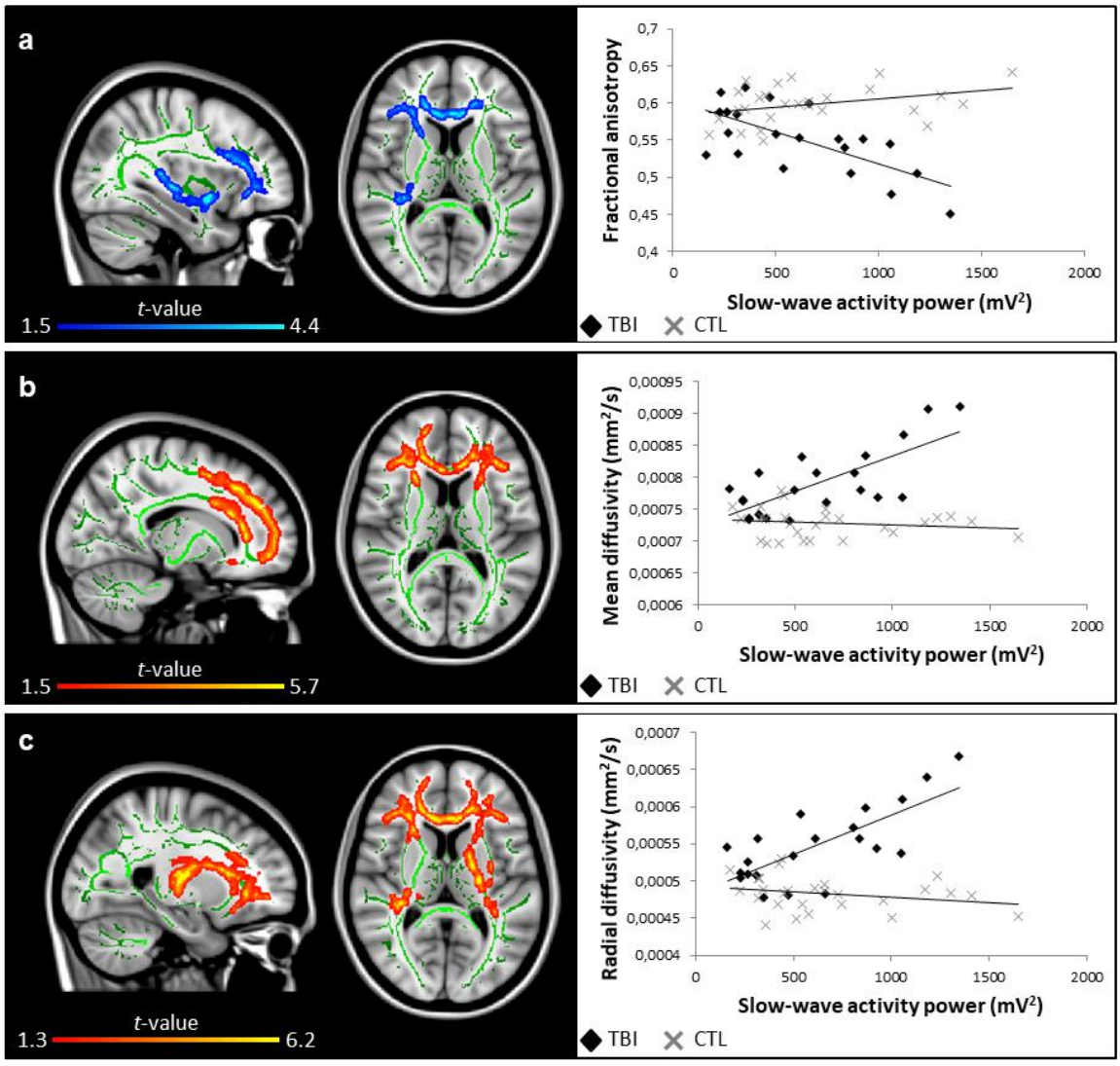

SUPPLEMENTARY FIGURE 3. Slow-wave activity power in the 2nd sleep cycle and white matter damage. Areas in traumatic brain injury (TBI) group where slow wave activity power is correlated (blue, negative correlation; red to yellow, positive correlation) with **(a)** fractional anisotropy (r = -0.63), **(b)** mean diffusivity (r = 0.60), and **(c)** radial diffusivity (r = 0.62). Significant results are overlaid over the MNI152 T1 1mm brain and the mean fractional anisotropy skeleton (in green). The correlation between the mean value of all significant clusters and slow-wave activity power is represented on the graphs. No significant correlation was found for the control group. Results are thresholded at p<0.05, adjusted for age and corrected for multiple comparisons.

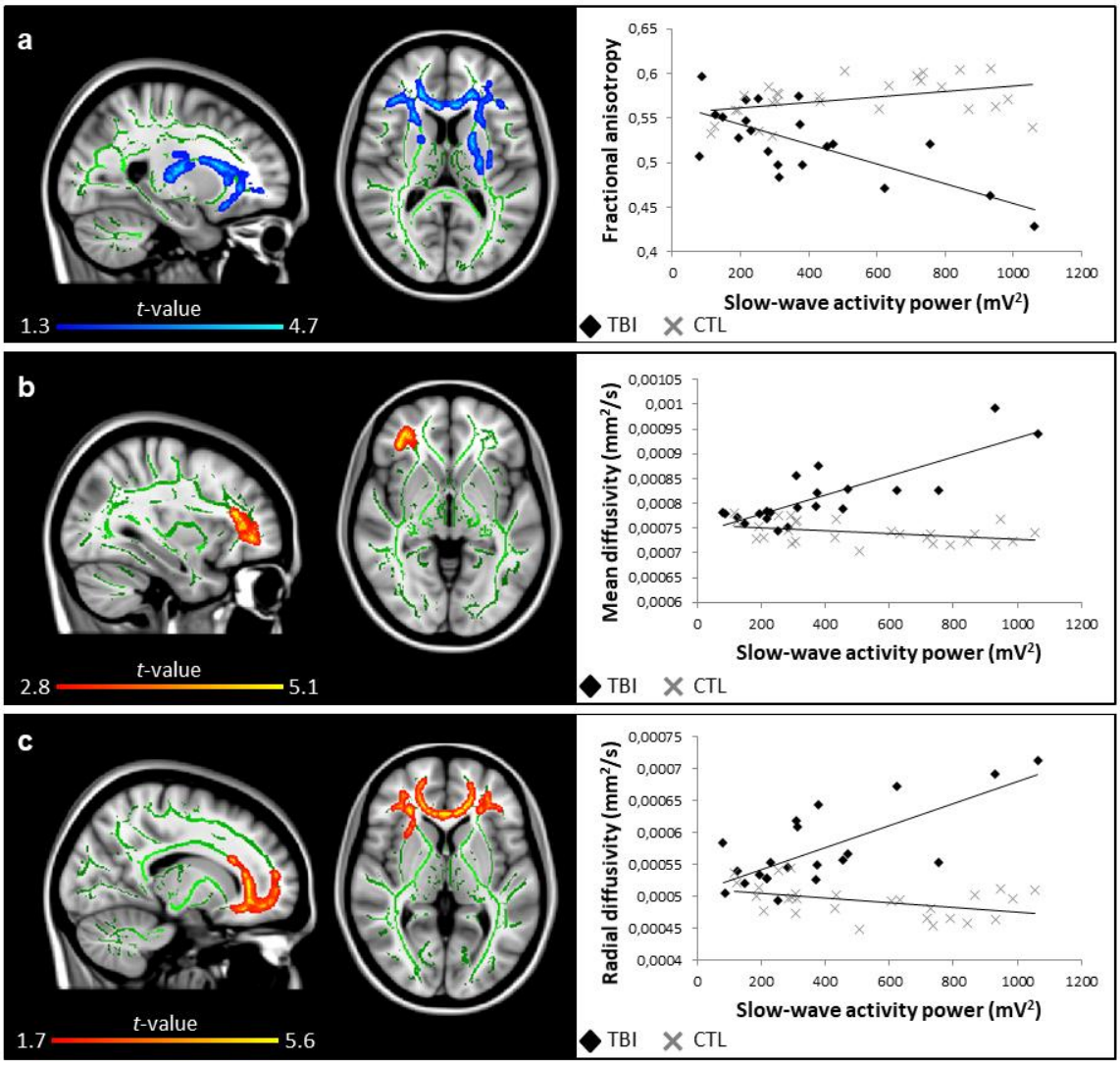

SUPPLEMENTARY FIGURE 4. Slow-wave activity power in the 3rd sleep cycle and white matter damage. Areas in traumatic brain injury (TBI) group where slow wave activity power is correlated (blue, negative correlation; red to yellow, positive correlation) with **(a)** fractional anisotropy (r = -0.69), **(b)** mean diffusivity (r = 0.80), and **(c)** radial diffusivity (r = 0.70). Significant results are overlaid over the MNI152 T1 1mm brain and the mean fractional anisotropy skeleton (in green). The correlation between the mean value of all significant clusters and slow-wave activity power is represented on the graphs. No significant correlation was found for the control group. Results are thresholded at $p<0.05$, adjusted for age and corrected for multiple comparisons.